PCCP

Accepted Manuscript

ROYAL SOCIETY OF CHEMISTRY

www.rsc.org/pccp

Investigation of nitriding and reduction processes in the nanocrystalline iron-ammonia-hydrogen system at 350°C

Bartlomiej Wilk[a], Walerian Arabczyk*[a]

[a] West Pomeranian University of Technology, Szczecin, Institute of Inorganic Chemical Technology and Environment Engineering, Pulaskiego 10, 70-322 Szczecin, Poland

*E-mail address: Bartlomiej.Wilk@zut.edu.pl

Abstract

In this paper, the series of phase transitions occurring during the gaseous nitriding of nanocrystalline iron was studied. Nitriding process of nanocrystalline iron and reduction process of the obtained nanocrystalline iron nitrides were carried out at 350°C in a tubular differential reactor equipped with systems for thermogravimetric measurement and analysis of gas phase composition. The samples were reduced with hydrogen at 500°C in the above mentioned reactor. Then the sample was nitrided at 350°C in a stream of ammonia-hydrogen mixtures of various nitriding potential, $P = p_{NH3}/p_{H2}^{3/2}$. At each nitriding potential stationary states were obtained – nitriding reaction rate is zero and catalytic ammonia decomposition reaction rate is constant. Reduction process of the obtained nanocrystalline iron nitrides was studied at 350°C in the stationary states as well. The phase composition of products obtained in both reaction directions (nitriding and reduction) was different despite identical concentration of nitrogen in the nitriding mixture. The hysteresis phenomenon, occurring in the iron nitriding degree – nitriding potential system, was explained. In the single-phase areas of α-Fe(N), γ'-Fe_4N or ε-$Fe_{3-2}N$, a state of chemical equilibrium between the ammonia-hydrogen mixture, nanocrystalline iron surface and volume was observed. In the multi-phase areas, between the gas phase and iron surface a state of chemical equilibrium holds, but between the gas phase and solid phase volume a state of quasi-equilibrium exists. The model of the nitriding process of nanocrystalline iron to iron nitride (γ'-Fe_4N) was presented. It was found, that nanocrystallites reacted in the order of their sizes from the largest to the smallest.

1. Introduction

Nitriding process of metals, in particular iron alloys, is widely carried out to improve the surface properties of nitrided materials. As a result of surface treatment of steels, their hardness, tensile strength and corrosion resistance is improved.[1-4] The surface modification of iron alloys now also is applied to improve the magnetic properties of the material.[3-7] Among the most commonly used methods of metal nitriding the following may be mentioned: gas[4,8] plasma[9] and fluorescent.[10]

On an industrial scale the gas nitriding of ferrous alloys is widely used to obtain a protective layer on their surfaces, consisting of iron nitrides. The nitriding reagent which is the most often used in this method is a gas mixture of ammonia and hydrogen.[11-13]

Studies on the thermodynamic equilibrium in the system iron-nitrogen-hydrogen were carried out by Lehrer, who described the boundaries of particular phases depending on the nitriding potential and temperature. Under given process conditions one can obtain single-phase iron nitrides - γ'-Fe_4N, ε-$Fe_{3-2}N$, ζ-Fe_2N[14,15] in the state of chemical equilibrium.

In recent years, increased interest in nanocrystalline materials is observed, including nanokrystalline iron nitrides, due to their different physicochemical properties compared to the materials of coarsely crystalline structure.[16-19] Nanocrystalline iron nitrides have magnetic properties, therefore, could potentially be used for the manufacture of magnets and electromagnets, magnetic heads of devices for magnetic data recording and in medical diagnosis as contrast agents.[9,17-21]

Studying the kinetics of the nitriding of nanocrystalline iron with ammonia, it was found that the reaction rate is limited by the rate of disassociative adsorption of ammonia on the surface of iron. Based on this finding a model of reaction in the adsorption range was elaborated.[22] From

this model it can be seen that the phase transition of nanocrystallites occurs in the order of their size, from the smallest to the largest.[23] New methods for determining the crystallite size distribution[24] and procedure for isolating the fraction of crystallites of a certain size[25] were developed.

Examining the nanocrystalline iron nitriding process and reduction of the obtained nitrides at temperatures of 400 to 500°C, it was found that the same nitriding degree of nanocrystalline iron in the reduction process is achieved at lower nitriding potentials than in the nitriding process. The phenomenon of hysteresis was observed in the system nitriding degree of iron-nitriding potential at constant temperature in stationary conditions.[26- 29]

In the system nanocrystalline iron-ammonia-hydrogen there were observed not only single-phase regions, but also mixtures of phases: α-Fe(N) + γ'-Fe_4N and γ'-Fe_4N + ε-$Fe_{3-2}N$,[30,31] what can not be explained on the basis of a well-known Lehrer's diagram.

The paper presents results of research on nanocrystalline iron nitriding process and reduction of the obtained nanocrystalline iron nitrides at 350°C in the stationary states. The influence of the nitriding mixture composition on the phase composition of products obtained in the processes of nitriding of nanocrystalline iron and nanocrystalline iron nitrides reduction was analyzed.

2. Experimental Methods

For investigations the industrial pre-reduced nanocrystalline iron catalyst for ammonia synthesis[32] was used. The iron catalyst precursor is formed by melting of magnetite ore with a little add of aluminum, calcium and potassium oxides in resistance furnace. Next, lava is cooled down, crushed and sieved to obtain selected fraction of grains. The catalyst precursor is reduced in hydrogen/nitrogen stream (3/1) in temperature of 500°C to obtained metallic, nanocrystalline

iron.[33] The nanocrystalline iron catalyst in this form is piroforic and before its unloading from the reactor, the passivation process need to be performed. After cooling the catalyst bed to temperature of 60°C at nitrogen stream, a little amount of air (about 0.75% ÷ 1.2%) to neutral gas flow was added.[34]

Chemical composition of the catalyst was determined by inductively coupled plasma – atomic emission spectrometry (ICP-AES) using a Perkin Elmer Optime 5300DV spectrometer (in wt%): 3.3 Al_2O_3, 2.8 CaO, 0.65 K_2O and 6.5 oxygen in the form of iron oxides. Philips X'Pert X-ray diffractometer with the copper lamp was used for the characterization of samples with various nitriding degrees. The average crystallite size of iron, as determined by Rietveld method, was 45 nm. To determine the specific surface area the Quadrasorb SI apparatus (Quantachrome Instruments, Automated Surface Area & Pore Size Analyzer) was applied. The specific surface area of the catalyst, determined by BET, was 12 m^2/g. A more detailed description of material used in the study has been presented in earlier publications. [35,36]

Nanocrystalline iron nitriding processes and reduction of obtained nanocrystalline iron nitrides were carried out in a differential tubular reactor equipped with a system that allows to perform the simultaneous thermogravimetric measurements (using a spring balance) and catharometric analysis of the hydrogen concentration in the gas phase. A sample of the catalyst by weight of 1.0 g and a grain size of 1.0 ÷ 1.2 mm was placed on a platinum basket in a form of single layer of grains. The nitriding process was preceded by a reduction of the passive layer of the catalyst. The reductions were carried out polythermally with the hydrogen flow of 9 dm^3/h, increasing the process temperature to 500°C at a rate of 5°C/min. The samples were annealed at this temperature until a stable weight was observed (approximately 30 min). Under these conditions, iron oxides contained in the catalyst were reduced, and the promoters remained in the oxide

form. During reduction pre-reduced nanocrystalline iron catalyst, the metallic iron was created in a form of nanocrystallites separated with structural promoters (Al_2O_3, CaO) bridges. The surface of nanocrystalline iron is wetted with K+O layer, where the iron atoms are covered directly by oxygen ions, and then with potassium. The oxygen layer is not completed as a result of geometric reason – diameter of potassium ion is so big that only every second Fe atom have been covered with oxygen. The surface of nanocrystals iron, 3D bridges of promoters and 2D layer of K+O are in chemical equilibrium, the surface and the bulk of nanocrystalline iron, as well.[37-39] Nitriding and reduction processes were carried out using gaseous ammonia having a purity of 99.98% and hydrogen with purity 99.999%. Gas flow rate was controlled by an electronic mass flow-meter placed at the inlet to the reactor. Changes in temperature and weight of the sample to be analyzed and the hydrogen concentration at the outlet of the reactor were recorded in a digital manner.

Studies of nanocrystalline iron nitriding process and reduction of obtained nanocrystalline iron nitrides were carried out isothermally at 350°C under atmospheric pressure by varying the composition of the nitriding mixture. The composition of the gas mixture was expressed as the partial pressure of components (p_{NH_3}, p_{H_2}) and then the nitriding potential can be described by the following equation:

$$P = \frac{p_{NH_3}}{p_{H_2}^{3/2}} \left[Pa^{-0.5} \right]$$

The change in mass of the sample was expressed as the nitriding degree, defined as the mass ratio of nitrogen contained in the sample, m_N, to the weight of iron contained in the same sample, m_{Fe}.

In order to analyse the phase composition and average crystallite size at the determined nitriding potentials, the carried out nitriding and reduction processes were stopped by a quickly cooling of the solid sample. The samples were cooled to a temperature below 50°C in the reactor in a stream of nitrogen and subjected to low temperature passivation by nitrogen with addition of oxygen (1.0 vol%). In the passivation process, the weight gain by approx. 1.0% was observed, corresponding to the formation of oxide layer with a thickness of approx. 1.5 nm on the surface of the nanocrystalline iron nitride. The resulting passive film thickness was comparable with literature data for iron catalyst.[40,41]

On the basis of X-ray diffraction (XRD) measurements the phase composition and average crystallite size of the obtained samples with different nitriding degrees were determined by the Rietveld method.

3. Results

Nanocrystalline iron nitriding process and reduction of obtained nanocrystalline nitrides were carried out at a temperature of 350°C at a varying composition of nitriding mixture. The mixtures of hydrogen and ammonia were introduced into the reactor, increasing the ratio NH_3:H_2 stepwise, during nitriding starting from pure hydrogen and ending for pure ammonia. During the process of reduction of nanocrystalline iron nitrides starting from pure ammonia or of the certain nitriding mixture and ending for pure hydrogen. Under these process conditions, the composition of the gas mixture at the reactor inlet was determined within the limits of measurement error ≈2%. After each change in the composition of the gas phase the process was carried out until steady state in which the rate of the nitridation reaction is zero (constant nitrogen content in the solid samples) was observed and the measured hydrogen concentration in the reactor was

constant. The steady states were already studied at higher temperatures.[26,42] Changing time of the gases in the reactor in relation to time to determine the steady state was relatively short, so that the composition of the gas phase in equilibrium was constant. In the case of a determination to one with of the stationary state, corresponding process conditions was kept constant for about 12 hours. No increase in mass of the sample was observed. There also changed the composition of the gas phase. Based on measurements of the hydrogen concentration at the inlet and outlet of the reactor, it was found that the rate of catalytic ammonia decomposition at a temperature of 350°C is negligible. Both in nanocrystalline iron nitriding process and reduction of obtained nanocrystalline nitrides, different nitriding degree stable at a steady-state corresponded to each pre-adjusted reaction mixture composition. In Figure 1, an exemplary dependence of the nitriding degree of solid sample and the hydrogen partial pressure over time for a fragment of one of the performed nanocrystalline iron nitriding processes is presented.

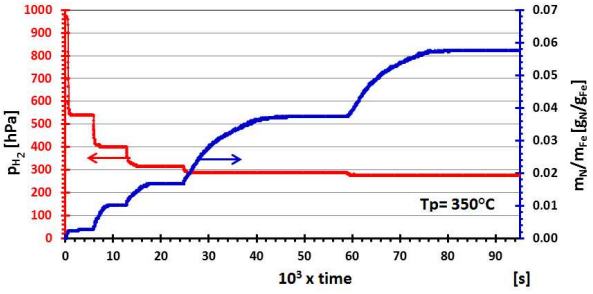

Figure 1. The changes of nitriding degree during the nitriding of nanocrystalline iron at 350°C with varying content of nitriding mixture. The partial pressure of hydrogen in the vicinity of the sample is depicted with a red line.

On the basis of a series of carried out experiments a dependence of nitriding degree on natural logarithm of nitriding potential at stationary states was developed (Figure 2) for nanocrystalline iron nitriding processes and reduction of obtained nanocrystalline iron nitrides. Values of

nitriding degree corresponding to the stoichiometric compositions of iron nitrides are marked by dashed horizontal lines. Characteristic points of the conducted processes are indicated by dashed vertical lines and above are given values of nitriding potential for these points.

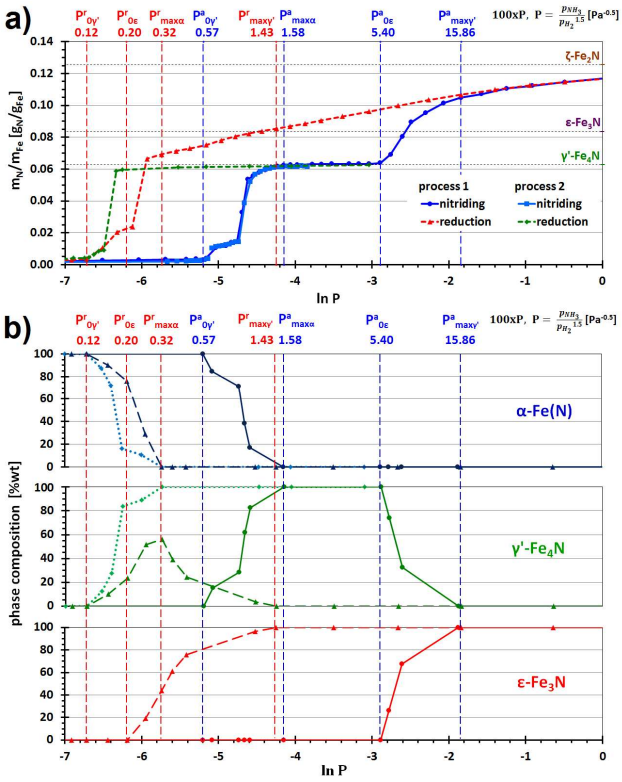

Figure 2. The dependence of the nitriding degree (a) and phase composition (b) on nitriding potential in the process of the nitriding of nanocrystalline iron (continuous line) and the reduction of the iron nitrides (dashed lines) at stationary states at 350°C: P – nitriding potential; a, r – as appropriate for nitriding process and reduction; α, γ ', ε - designation of phases α-Fe (N), γ'-Fe_4N and ε-$Fe_{3-2}N$; 0, max - as appropriate for the minimum and maximum nitriding potential at which exists a phase.

In this figure also a comparative study of the nanocrystalline iron nitriding process and reduction of obtained nanocrystalline iron nitrides at 350°C is shown, taking into account different final nitriding potentials. Process No. 1 was carried out to achieve a maximum nitriding

degree (conversion: α-Fe(N) → γ'-Fe_4N → ε-$Fe_{3-2}N$). Process No. 2 was carried out until the nitriding degree of solid samples was corresponding to the stoichiometric composition of Fe_4N (conversion: α-Fe(N) → γ'-Fe_4N).

In order to determine the phase composition and an average crystallite size of each of the compounds produced in the process No. 1 at certain nitriding potentials and the corresponding nitriding degrees in the stationary states, the processes in question were stopped. Nitrided samples were passivated and their diffraction patterns were obtained. Selected diffraction patterns for the nanocrystalline iron nitriding process are shown in Figure 3a, and for the reduction process of nanocrystalline iron nitrides in Figure 3b. Phase analysis was performed using the X'Pert HighScore Plus program, based on crystallographic data contained in the identification cards database ICDD PDF-4+. For the phase analysis the cards of indices: 04-004-2482 for α-Fe phase, 04-004-9107 for γ'-Fe_4N phase and 04-007-2960 for phase ε-Fe_3N were used. Based on the identification cards, peaks corresponding to particular phases were marked with dotted vertical lines of different colors on the diffraction patterns. For each diffraction pattern the nitriding degree obtained during the process, nitriding potential at which the process was stopped and the phases present in the sample are also given.

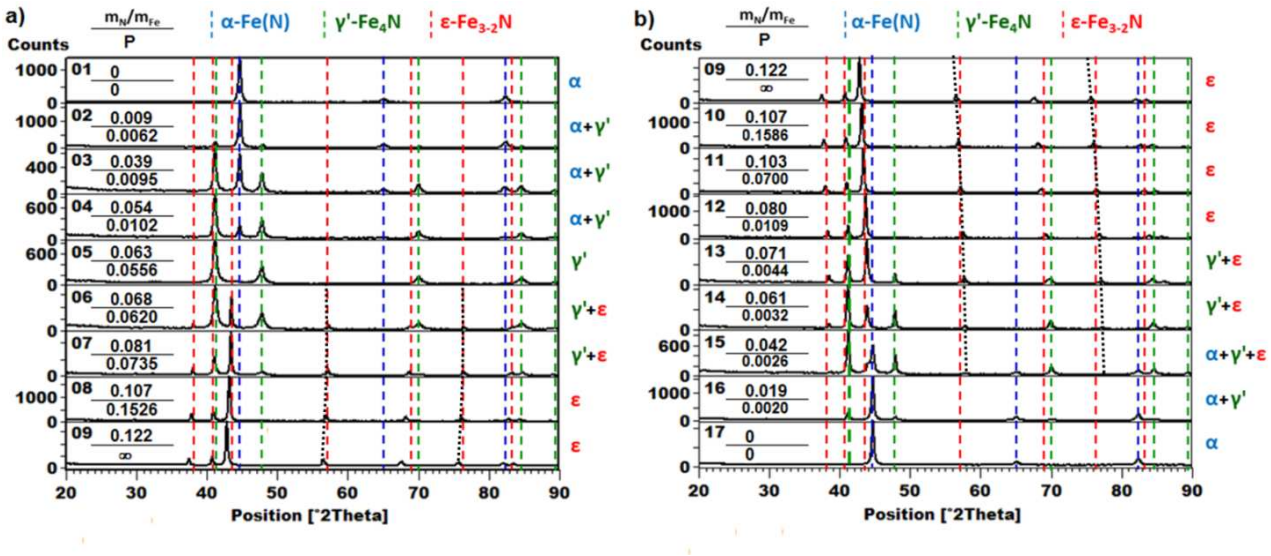

Figure 3. Diffractograms for the materials obtained at 350°C in the process the nitriding of nanocrystalline iron (a) and the reduction of the iron nitrides (b).

Execution the nanocrystalline iron nitriding process (diffraction pattern No. 01) below the minimum level of nitriding potential, small nitriding degree amounting to 0.004 g_N/g_{Fe} was obtained. At this stage of the process, a solution of nitrogen in nanocrystalline iron, α-Fe(N) is formed, with nitrogen adsorbed on its surface is.[43] After crossing $P^a_{0\gamma'}$, the nitriding degree increases non-monotonically to a value corresponding to the stoichiometric composition of the Fe_4N compound, at the maximum nitriding potential, $P^a_{max\alpha}$ at which phase α-Fe(N) is still stable. The change in the phase composition in this range of potentials is observed on diffractograms 02 ÷ 04, where there are peaks of α-Fe(N) and γ'-Fe_4N phases. The intensity of α-Fe(N) peaks is decreasing, and of the characteristic peak for γ'-Fe_4N is increasing, which results from the decreasing content of iron and a growing γ'-Fe_4N nitride content. From the nitriding potential value $P^a_{max\alpha}$ to the minimum nitriding potential $P^a_{0\varepsilon}$, at which ε-$Fe_{3-2}N$ phase is formed, a slight increase in the nitriding degree (plateau on the nitriding curve) is observed in a

wide range of potentials. On the diffraction pattern No. 05 for the sample obtained in this range of nitriding potentials, peaks characteristic only for the γ'-Fe_4N phase are observed. When increasing the nitriding potential above $P^a_{0\varepsilon}$, a monotonic increase in the nitriding degree to a level corresponding to the maximum content of nitrogen in the sample, $m_N/m_{Fe} = 0.12\ g_N/g_{Fe}$, is observed. In this range of potentials, to $P^a_{max\gamma'}$ two phases, γ'-Fe_4N and ε-$Fe_{3-2}N$, are stable in the sample – diffraction patterns Nos. 06 and 07, and above $P^a_{max\gamma'}$ only ε-$Fe_{3-2}N$ phase lasted – diffraction patterns 08 and 09.

In the process of reduction of nanocrystalline iron nitrides obtained during the process No. 1, nitriding degree of iron decreases monotonically with a change in nitriding potential from a maximum value ($m_N/m_{Fe} = 0.12\ g_N/g_{Fe}$) to a value slightly above the stoichiometric chemical composition of γ'-Fe_4N ($m_N/m_{Fe} = 0.07\ g_N/g_{Fe}$), at the nitriding potential 0.0027 $Pa^{-0.5}$. In the diffractograms 09÷11, for samples reduced with hydrogen-ammonia mixtures of nitriding potentials above $P^r_{max\gamma'}$, only peaks of ε-$Fe_{3-2}N$ phase are observed, and diffraction patterns 12 and 13 (for the samples prepared below nitriding potential $P^r_{max\gamma'}$) contain, apart from characteristic peaks of the ε-$Fe_{3-2}N$ phase, peaks corresponding to γ'-Fe_4N phase. On further lowering of the minimum nitriding potential to $P^r_{0\gamma'}$, decraese in the value of the nitriding degree down to a level corresponding to the solution of nitrogen in nanocrystalline iron α-Fe(N) is observed. Diffraction patterns 14÷16 obtained for samples prepared at nitriding potentials from this range. In the diffractogram 14, peaks characteristic for ε-$Fe_{3-2}N$ and γ'-Fe_4N phase are observed, in the diffractogram 15 additionally peaks characteristic to α-Fe(N) phase occur, and in the diffractogram 16 peaks characteristic to γ'-Fe_4N and α-Fe(N) phases can be seen. Decrease in potential to less than $P^r_{0\gamma'}$ resulted in a further decrease in nitriding degree until the value

corresponding to the solution of hydrogen in nanocrystalline iron α-Fe(H) – diffraction pattern 17, on which only peaks characteristic for α-Fe were observed.

For ε-$Fe_{3-2}N$ phase, diffraction peak shifts towards lower reflection angles in the nanocrystalline iron nitriding process and towards higher angles of reflection in the reduction of nanocrystalline iron nitrides are observed (black dashed lines in Figure 3). There were no significant changes at the position of diffraction reflections for α-Fe(N) and γ'-Fe_4N phases. Changes in the position of diffraction reflections are the result of changes in lattice constant, as a result of varying nitrogen content in the crystal structure of a given compound. In the case of α-Fe(N) and γ'-Fe_4N phases, in which the nitrogen content in the crystal lattice structure varies to a small extent, changes in the position of the peaks are not as noticeable as in the case of ε-$Fe_{3-2}N$ phase for which the nitrogen content in the crystal lattice structure varies widely. The values of lattice constants of ε-$Fe_{3-2}N$ phase are changing in the following manner. Lattice constant ***a*** in the nitriding process increases by 0.0753 Å in the range of from 4.7265 to 4.8018 Å and for lattice constant ***c*** increases about value 0.0310 Å from 4.3950 Å to 4.4260 Å. In the process of reducing the value of both lattice constant decreases, for lattice constant ***a*** about value 0.1487 Å from 4.8018 Å to 4.6531 Å and for lattice constant ***c*** by 0.0535 Å in the range of from 4.4260 Å to 4.3725 Å. The values of both lattice constants ε-$Fe_{3-2}N$ phase in the final reduction stage of this phase were lower than during the formation of this phase during the nitriding process. In the reduction process, phase ε-$Fe_{3-2}N$ below the nitriding potential $P^r_{max\gamma'}$ can achieve chemical composition corresponding to compound ε-Fe_4N.

Dependence of the nitriding degree on nitriding potential for the reduction process of nanocrystalline nitrides obtained during the nitriding process carried out to the nitriding degree close to the stoichiometric composition of γ'-Fe_4N compound proceeds in a different way than in

the case of nitrides obtained during the process conducted to ε-$Fe_{3-2}N$ (the maximum nitriding degree m_N/m_{Fe} = 0.12 g_N/g_{Fe}). In the reduction process, for which the output phase was nanocrystalline γ'-Fe_4N nitride, in the nitriding potential range from 0.0540 $Pa^{-0.5}$ to 0.0016 $Pa^{-0.5}$ the nitriding degree decreases slightly (approximately 0.004 g_N/g_{Fe}). In the potential range from 0.0016 $Pa^{-0.5}$ to a minimum nitriding potential in the process of reduction, $P^r_{0\gamma'}$, at which γ'-Fe_4N phase is still stable, decrease in the nitriding degree is observed from the value close to the stoichiometric composition of γ'-Fe_4N to the value of nitriding degree characteristic for solution of nitrogen in the nanocrystalline iron α-Fe(N). While decreasing the nitriding potential below $P^r_{0\gamma'}$, a further decrease in the nitriding degree occurs until the value corresponding to the solution of hydrogen in nanocrystalline iron α-Fe(H) is achieved.

For three ranges of potentials: less than $P^a_{0\gamma'}$, from $P^a_{max\alpha}$ to $P^a_{0\varepsilon}$ and above $P^a_{max\gamma'}$ the nitriding mixture composition was changed towards higher and lower potentials. Regardless of which direction was changed the nitriding potential the same dependence of the nitriding degree of sample on nitriding potential was observed.

For the reduction process of obtained nanocrystalline iron nitrides the dependence of the nitriding degree of the sample on nitriding potential does not match with an analogous relationship for the nanocrystalline iron nitriding process. In the range of nitriding potentials where two phases coexist, isotherm for nanocrystalline iron nitrides reduction process extends above the isotherm for nitriding process. For the iron nitriding processes and reduction of nanocrystalline iron nitrides obtained at a temperature of 350°C, the hysteresis effect was observed. As a result of multiple repetition of nitriding and reduction processes, the same hysteresis curves were obtained. Based on this observation it can be concluded that the morphology and chemical composition of the iron catalyst does not change. Based on these

findings, one can say that the iron catalyst in single-phase areas reaches the states of chemical equilibrium, and in two- and three-phase areas the catalyst is in the states of chemical quasi-equilibrium.

On the basis of the obtained diffraction patterns, phase composition and the average crystallite size of α-Fe and γ'-Fe_4N were calculated by Rietveld method for each sample treated with a nitriding mixture.

Figure 2b shows the changes in the content of the various nanocrystalline phases with the change in the nitriding potential of gas mixture. Nitriding potential values corresponding to the characteristic steps of the nanocrystalline iron nitriding reaction and reduction of the obtained nanocrystalline iron nitrides are marked with dotted vertical lines. A detailed description for the selected values of nitriding potentials is given in Table 1. For the α-Fe(N) and γ'-Fe_4N phases additionally changes in the content of individual phases for the reduction process conducted from the obtained γ'-Fe_4N phase. For this process the hysteresis effect in the area of coexistence of phases α-Fe(N) and γ'-Fe_4N was observed. For the conversion, where the nanocrystalline iron was nitrided through the γ'- Fe_4N to ε-$Fe_{3-2}N$, the hysteresis phenomenon was observed for the area of occurrence of phase α-Fe(N) and ε-$Fe_{3-2}N$.

Based on the results shown in Figure 3a and 2b an analysis of the phase composition changes during the nanocrystalline iron nitriding at 350°C was performed. The phase composition of the material under consideration was changing with the process from the solid solution of nitrogen in nanocrystalline iron through the mixture of iron saturated with nitrogen and iron nitride γ'-Fe_4N, a mixture of nitrides γ'-Fe_4N and ε-$Fe_{3-2}N$, up to ε-$Fe_{3-2}N$ phase with varying degree of saturation with nitrogen. Areas of existing of particular phases and their mixtures with respect to the

nitriding potential and nitriding degree are shown in Table 1. Presence of two phases at a given nitriding degree during the nanocrystalline iron nitriding process was stated.

Table 1. Nitriding potentials corresponding to characteristic stages of nitriding the nanocrystalline iron and reduction of the nanocrystalline iron nitrides at 350°C

The process of the nitriding of nanocrystalline iron			
Ranges of potentials	**Nitriding potentials P [$Pa^{-0.5}$]**	**Nitriding degree m_N/m_{Fe} [g_N/g_{Fe}]**	**Phases occurring**
$< P^a_{0\gamma'}$	< 0.0057	< 0.004	α-Fe(N)
$P^a_{0\gamma'} - P^a_{max\alpha}$	0.0057 ÷ 0.0158	0.004 ÷ 0.063	α-Fe(N), γ'-Fe_4N
$P^a_{max\alpha} - P^a_{0\varepsilon}$	0.0158 ÷ 0.0540	0.063	γ'-Fe_4N
$P^a_{0\varepsilon} - P^a_{max\,\gamma'}$	0.0540 ÷ 0.1586	0.063 ÷ 0.102	γ'-Fe_4N, ε-$Fe_{3-2}N$
$> P^a_{max\,\gamma'}$	> 0.1586	0.102 ÷ 0.122	ε-$Fe_{3-2}N$
The process of the reduction of the iron nitrides at process No. 1			
Ranges of potentials	**Nitriding potentials P x 10^2 [$Pa^{-0.5}$]**	**Nitriding degree m_N/m_{Fe} [g N/g Fe]**	**Phases occurring**
$> P^r_{max\gamma'}$	> 0.0143	0.122 ÷ 0.084	ε-$Fe_{3-2}N$
$P^r_{max\gamma'} - P^r_{max\alpha}$	0.0143 ÷ 0.0032	0.084 ÷ 0.063	ε-$Fe_{3-2}N$, γ'-Fe_4N
$P^r_{max\alpha} - P^r_{0\varepsilon}$	0.0032 ÷ 0.0020	0.063÷ 0.024	ε-$Fe_{3-2}N$, γ'-Fe_4N, α-Fe(N)
$P^r_{0\varepsilon} - P^r_{0\gamma'}$	0.0020 ÷ 0.0012	0.024 ÷ 0.004	γ'-Fe_4N, α-Fe(N)
$< P^r_{0\gamma'}$	< 0.0012	< 0.004	α-Fe(N)
The process of the reduction of the iron nitrides at process No. 2			
Ranges of potentials	**Nitriding potentials P x 10^2 [$Pa^{-0.5}$]**	**Nitriding degree m_N/m_{Fe} [g N/g Fe]**	**Phases occurring**
$> P^r_{max\alpha}$	> 0.0032	0.062 ÷ 0.060	γ'-Fe_4N
$P^r_{max\alpha} - P^r_{0\gamma'}$	0.0032 ÷ 0.0012	0.060 ÷ 0.006	γ'-Fe_4N, α-Fe(N)
$< P^r_{0\gamma'}$	< 0.0012	< 0.006	α-Fe(N)

$P^a_{0\gamma'}$ – minimum nitriding potential in the process of nitriding, at which γ'-Fe_4N phase is formed,
$P^a_{max\alpha}$ – maximum nitriding potential in the process of nitriding, at which α-Fe(N) phase is still,
$P^a_{0\varepsilon}$ – minimum nitriding potential in the process of nitriding, at which ε-$Fe_{3-2}N$ phase is formed,
$P^a_{max\,\gamma'}$ – maximum nitriding potential in the process of nitriding, at which γ'-Fe_4N phase is still,
$P^r_{max\gamma'}$ – maximum nitriding potential in the process of reduction, at which γ'-Fe_4N is formed,
$P^r_{max\alpha}$ – maximum nitriding potential in the process of reduction, at which α-Fe(N) is formed,
$P^r_{0\varepsilon}$ – minimum nitriding potential in the process of reduction, at which ε-$Fe_{3-2}N$ phase is still,
$P^r_{0\gamma'}$ – minimum nitriding potential in the process of reduction, at which γ'-Fe_4N phase is still.

Based on the diffraction patterns shown in Figure 3b, the phase composition of the samples in the reduction of nanocrystalline iron nitride ε-$Fe_{3-2}N$ at 350°C was determined (Figure 2b). There was observed a conversion of ε-$Fe_{3-2}N$ phase, with the highest degree of saturation with nitrogen (maximum obtained nitriding degree), through the ε-$Fe_{3-2}N$ phase less saturated with nitrogen, a mixture of two nitrides γ'-Fe_4N and ε-$Fe_{3-2}N$, a mixture of three phases: α-Fe(N), γ'-Fe_4N, ε-$Fe_{3-2}N$, a mixture of two nitrides γ'-Fe_4N and α-Fe(N) to the α-Fe(H) phase in the sample after the complete decomposition of iron nitrides. Based on the results of quantitative phase analysis, presented in Figure 2b, coexistence of three phases was observed for the samples reduced in nitriding mixtures within the range $P^r_{max\alpha}$-$P^r_{0\varepsilon}$. Along with the progress of the reduction process a decrease in the content of ε-$Fe_{3-2}N$ phase was observed below $P^r_{max\gamma'}$, first to γ'-Fe_4N nitride, and then also to α-Fe(N).

Based on powder diffraction patterns for the nanocrystalline iron nitriding process, the average crystallite sizes of α-Fe(N) and γ'-Fe_4N while taking into account the lattice strain were determined by the Rietveld method. The obtained dependence of the average crystallite size and the lattice strain on the nitriding degree is shown in Figure 4. In the determination of these parameters into account deconvolution of simultaneously size and strain tems. The average crystallite sizes of both α-Fe(N) as well as γ'-Fe_4N decrease with increasing nitriding degree. and the lattice strain of both this phases slightly increase with increasing nitriding degree. Changes in the lattice strain are associated with the incorporation of a further nitrogen atoms in the structure of the individual phases.

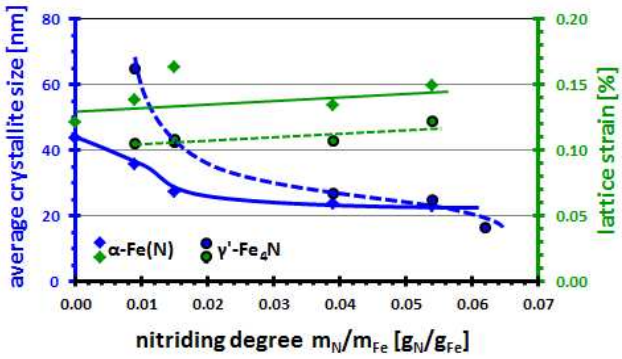

Figure 4. The dependence of average crystallite size and lattice strain on the nitriding degree in the process of the nitriding of nanocrystalline iron to γ'-Fe_4N phase.

Based on the dependence on nitriding potential in the process of the nitriding of nanocrystalline iron to γ'-Fe4N phase, the dependence of weight gain on nitriding degree was determined (Figure 5).

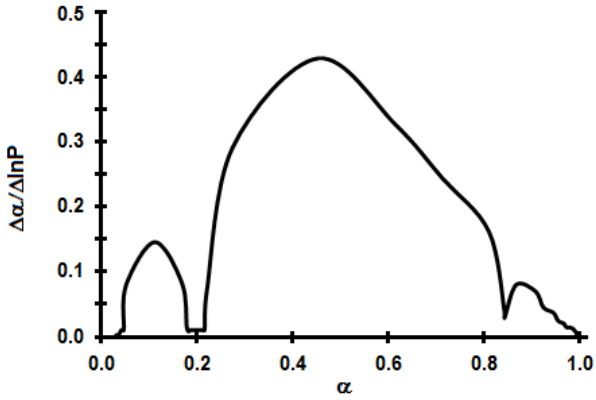

Figure 5. The dependence Δα/ΔdlnP of the nitriding level in the process of the nitriding of nanocrystalline iron.

This dependence was used to determine the size distribution of crystallite (GSD) according to the method proposed by Pelka in article.[44] For this purpose, on the basis of microscopic observations SEM iron catalyst, was assumed the size of the nanocrystallites as 10-70 nm and a shape factor S/V as for the sphere. The shares of individual fractions were chosen in such a way that area under the curve GSD=f(d) was equal to unity for the specified range of diameters of

crystallites. The average diameter size calculated based on the acquired GSD was equal to the average diameter obtained by XRD. The probability of occurrence of a particular fraction of crystallites in the catalyst has been calculated and their size distribution (GSD) has been specified. The obtained size distribution was compared with results obtained by means of XRD method (after Pielaszek) and BET method (Figure 6).

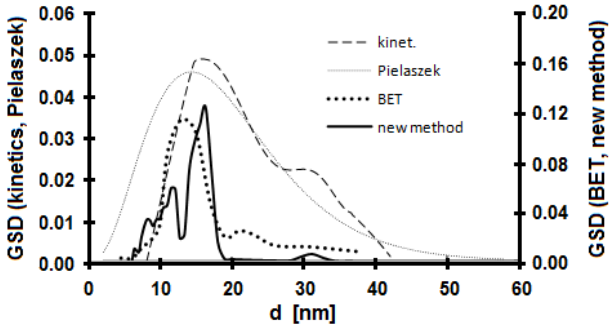

Figure 6. Crystallite size distribution indicated by various methods for the process of the nitriding of nanocrystalline iron.

4. Discussion

Examining the process of ammonia synthesis over iron catalyst it was hypothesized that the iron catalyst in the ammonia synthesis process is in a state of chemical equilibrium[39] and an attempt was made to demonstrate that multicomponent nanocrystalline materials whose surface is coated with a two-dimensional structure of the adsorbent may be in a state of chemical equilibrium.[44] The results presented in this work show plausible the hypothesis outlined earlier.

During the catalytic decomposition of ammonia on iron catalyst the stationary states exist in which there is only the ammonia decomposition reaction and a state of chemical equilibrium is established between the chemical potential of a nitriding mixture and the chemical potential in the volume of iron nanocrystallites and iron nitrides. Along with increase in the nitriding

potential the single-phase areas are observed: α-Fe(N), γ'-Fe_4N, ε-$Fe_{3-2}N$ and the areas of coexistence of two phases: α-Fe(N) + γ'-Fe_4N and γ'-Fe_4N + ε $Fe_{3-2}N$, as observed in previous studies on nitriding process of the catalyst at higher temperatures.[26-29] In the reduction process of the nanocrystalline nitride ε-$Fe_{3-2}N$ at a temperature of 350°C it was observed, in addition to the aforementioned single- and two-component areas, the area of coexistence of three solid phases: α-Fe(N) + γ'-Fe_4N + ε-$Fe_{3-2}N$ in the range of potentials from 0.0032 $Pa^{-0.5}$ to 0.0020 $Pa^{-0.5}$. The occurrence range of particular phases and mixtures thereof of nitriding nanocrystalline iron and reduction of the obtained nanocrystalline iron nitrides at 350°C on the Lehrer's diagram by colored lines was marked (Fig. 7). Areas the coexistence of two phases in the process of nitriding (Fig. 7a) and the coexistence of three phase in the reduction process (Fig. 7b) are marked by colorful fields. On the Lehrer's diagram also marked literature data on previously conducted processes at higher temperatures.[26,45-47]

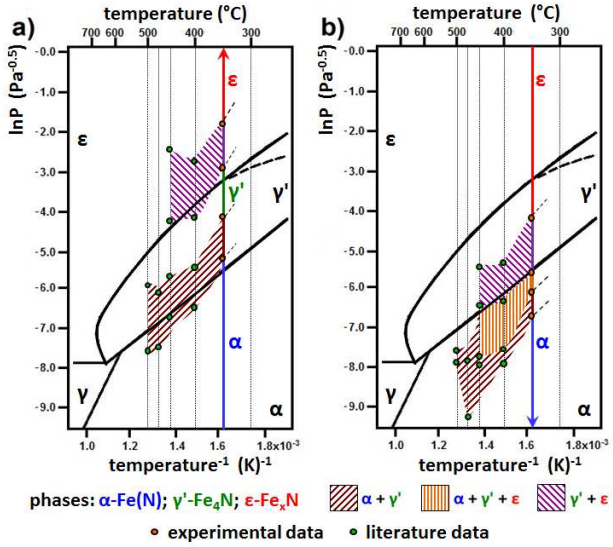

Figure 7. Comparison of the experimental data and the results of various studies creating the Lehrer diagram, for the process of the nitriding of nanocrystalline iron (a) and the reduction of the iron nitrides (b).

Studying the nitriding process and ammonia decomposition at 475°C the dependences of ammonia decomposition rate on the nitriding potential in the stationary states were determined. In the potentials area corresponding to the existence of a solution of nitrogen in the iron, α-Fe(N), the rate of catalytic decomposition of ammonia increases and in the nitriding potential areas corresponding to the coexistence of two phases α-Fe(N) and γ'-Fe_4N and the existence of γ'-Fe_4N phase the rate of catalytic decomposition of ammonia decreases.[42] The determined ammonia decomposition rates are independent of the direction of potential changes, what proves that in the entire range of nanocrystalline iron nitriding process and reduction of nanocrystalline nitride a state of chemical equilibrium holds between the volume and the surface of the catalyst.

In the stationary states in the single-phase areas of α-Fe(N), γ'-Fe_4N and ε-$Fe_{3-2}N$ a state of chemical equilibrium exists between the ammonia-hydrogen mixture, the catalyst surface and solid phase. In the multi-phase areas a state of chemical equilibrium holds between the gas phase and the catalyst surface and the quasi-equilibrium state between the gas phase and solid phase volume.

The observed hysteresis phenomena can be explained by the different energetic effects occurring during the nanocrystalline iron nitriding process and reduction of the obtained nanocrystalline iron nitrides.

Let us consider the phenomena occurring in the process of nitriding of a single nanocrystallite. Creating of a solution of nitrogen in iron is an endothermic process. Along with increase in the chemical potential of nitrogen in nanocrystallite volume its energy increases. The rate of the nitriding process is very small compared to the rate of diffusion processes taking place within the nanocrystallite, thus in the entire volume of the crystallite a uniform concentration of nitrogen occurs. After reaching the critical concentration of nitrogen in the α-Fe(N) solution, when the

energy of the nanocrystallite is sufficient to transform the bcc sublattice of α-Fe phase (α-nitro-ferrite) into the fcc sublattice of γ-Fe a recrystallization of bcc sublattice takes place, which results in a thermodynamically unstable structure of γ-Fe(N) (γ-austenite) with a low nitrogen content. Unsaturated γ-Fe(N) solution is rapidly saturated to form γ'-$Fe_{4-X_{min}}N$ compound. This compound is a non-stoichiometric one with its composition close to Fe_4N, in which the nitrogen chemical potential is in a state of chemical equilibrium with the nitriding potential of a nitriding mixture. The value of X parameter depends on the nitriding potential at a given temperature. Along with an increase in the nitriding potential of the gas mixture the value of X decreases and Fe_4N compound is formed. With a further increase in the potential, similarly as with the conversion of α-Fe(N) → γ'-Fe_4N, the following transformation process occurs: γ'-Fe_4N → ε-$Fe_{3-Y}N$, where Y<1. Iron fcc sublattice of γ'-Fe_4N phase transforms into the hcp sublattice of ε phase. The chemical composition of ε phase can be considered as a solution in a wide range of nitriding degree 0.043 g_N/g_{Fe} ÷ 0.123 g_N/g_{Fe},[48] which depends on the nitriding potential. After the transformation of γ'-Fe_4N phase into the unstable ε-Fe_4N phase, which becomes saturated at a chemical equilibrium state increasing the nitriding degree up to Fe_3N corresponding to the nitriding potential $P^a_{max\gamma}$'.

In the nanocrystalline iron nitriding process ζ-Fe_2N phase was not obtained.

Based on the results shown in Figure 2, it was found that the process of reduction of nanocrystalline iron nitrides proceeds differently depending on the initial nitriding degree of the sample corresponding to γ'-Fe_4N or ε phase (m_N/m_{Fe} = 0.12 g_N/g_{Fe}).

In the reduction process of γ'-Fe_4N along with a decrease in the nitriding potential of the gas phase the nitrogen concentration in $Fe_{4-X}N$ decreases as well. This process is associated with the process of creation of defects in the bcc crystal lattice leading to increased energy of

nanocrystallite. Upon the recrystallization of γ'-Fe sublattice the energy of the sublattice recrystallization is released, which balances the formation of the thermodynamically unstable supersaturated α'-Fe(N) phase with the chemical composition of $Fe_{4-X_{min}}N$ (α'-martensite), which as a result of further removal of nitrogen from the surface of the sample goes into equilibrium state of α-Fe(N).

In the process of reduction of ε phase along with decreasing in the nitriding potential the nitrogen concentration of the ε phase decreases to the nitriding degree equal to approx. 0.065 g_N/g_{Fe} (ε-$Fe_{2+Z}N$) at the nitriding potential $P^r_{max\alpha}$. Starting from the nitriding potential $P^r_{max\gamma'}$, apart from ε phase the γ'-Fe_4N phase exists. Below nitriding potential $P^r_{max\alpha}$, three phases exist in the system: α-Fe(N), γ'-Fe_4N and ε-$Fe_{2+Z}N$. One can hypothesize that at potential $P^r_{max\alpha}$ direct conversion process of ε-$Fe_{2+Z}N$ phase to α-Fe(N) takes place.

Taking into account the dependence of the average crystallite size on the nitriding degree (Figure 4), which shows that the crystallite size of the substrate and the product decreases with an increase in the nitriding degree of iron, it should be noted that the order of reacted crystallites depends on their size and they reacted in the order from the largest to the smallest (Figure 8). This phenomenon was used to determine the crystallite size distribution of iron catalyst.[24]

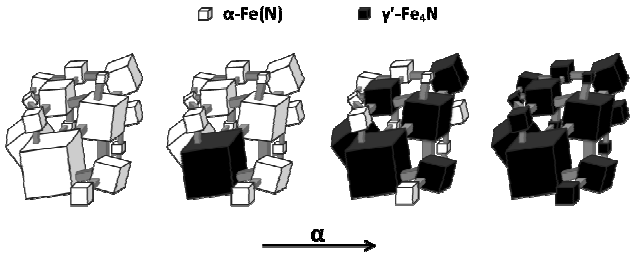

Figure 8. The model of the nitriding process of nanocrystalline iron until obtained the iron nitrides γ'-Fe_4N.

The observed areas of the coexistence of two phases can be explained by differences in the size of iron nanocrystallites and the obtained iron nitrides, and therefore also different values of the nitriding potential necessary for the occurrence of a phase transition of individual crystallites.[45,49]

5. Conclusions

In the nanocrystalline iron nitriding process and reduction of the obtained iron nitrides the hysteresis phenomenon is observed. In the stationary states in the areas of single-phase of α-Fe(N), γ'-Fe_4N and ε-$Fe_{3-2}N$ a state of chemical equilibrium exists between the ammonia-hydrogen mixture, catalyst surface and solid phase. In the multi-phase areas a state of chemical equilibrium holds between the gas phase and catalyst surface and the state of quasi-equilibrium exists between the gas phase and solid phase volume. In the process of nitriding in quasi-equilibrium states coexist two phases α-Fe(N) + γ'-Fe_4N and γ'-Fe_4N + ε-$Fe_{3-2}N$, and in the reduction process apart from the two-component systems the ternary system α-Fe(N) + γ'-Fe_4N + ε-$Fe_{3-2}N$ is observed as well.

In the nitriding process, at the nitriding potential gradually increasing, crystallites undergo a phase transition throughout their volume and in the order of their size, from the largest to the smallest.

AUTHOR INFORMATION

Corresponding Author

*E-mail: Bartlomiej.Wilk@zut.edu.pl

Author Contributions

The manuscript was written through contributions of all authors. All authors have given approval to the final version of the manuscript.

Notes

The authors declare no competing financial interest.

ACKNOWLEDGMENT

The scientific work was financed by The National Centre for Research and Development - program 'Lider', project No. LIDER/025/489/L-5/13/NCBR/2014. Special thanks to Dr. Rafal Pelka for fruitful discussions.

REFERENCES

1. J.M. Lakhtin, J.D. Kogan, *Azotirovanie stali*, Maśinostroenie, Moskwa, 1976.
2. H.T. Chen, M.F. Yan, Y. You, *J. Magn. Magn. Mater.,* 2014, 354, 200-204.
3. Ö. Alpaslan, E. Atar, H. Çimenoğlu, *JESTECH,* 2012, 15, 39-43.
4. J. Wendland, J. Borowski, L. Maldzinski, *Obrobka Plastyczna Metali,* 2011, 22, 75-82.
5. J.M.D. Coey, P.A.I. Smith, *J. Magn. Magn. Mater*., 1999, 200, 405-424.
6. M. Kano, T. Nakagawa, T.A. Yamamoto, M. Katsura, *J. Alloys Comp*., 2001, 327, 43-46.
7. Y.R. Jang, I.G. Kim, J.I. Lee, *J. Magn. Magn. Mater*., 2003, 263, 366-372.
8. B. Pachutko, L. Maldzinski, *Obrobka Plastyczna Metali,* 2011, 22, 227-243.
9. R. Zulhijah, K. Yoshimi, A.B.D. Nandiyanto, T Ogi, T. Iwaki, K. Nakamura, K. Okuyama, *Adv. Powder Technol.,* 2014, 25, 582-590.
10. T. Fraczek, C. Kolmasiak, M. Olejnik, Z. Skuza, *Metalurgija*, 2011, 50, 97-100.
11. D.K. Inia, A.M. Vredenberg, F.H.P.M. Habraken, D.O. Boerma. *J. Appl. Phys*., 1999, 86, 810-816.
12. K. Nishimaki, S. Ohmae, T.A. Yamamoto, M. Katsura, *NanoStruct. Mater.*, 1999, 12, 523-526.
13. J.F. Gu, D.H. Bei, J.S. Pan, J.Lu, K. Lu, *Mater. Lett.,* 2002, 55, 340-343.
14. E. Lehrer, *Z. Electrochem*., 1930, 36, 383-392.
15. J. Kunze, *Nitrogen and carbon in iron and steel thermodynamics*., Akademie-Verlag: Berlin, 1990.

16. E.P. Wohlfarth., *Pure Appl. Chem*. 1985, 57, 1403-1406.
17. H. Nakajima, Y. Ohashi, K. Shiiki, *J. Magn. Magn. Mater*., 1997, 167, 259-263.
18. S. Bhattacharyya, S.M. Shivaprasad, N.S. Gajbhiye, *Chem. Phys. Lett*., 2010, 496, 122-127.
19. Z. Schnepp, M. Thomas, S. Glatzel, K. Schlichte, R. Palkovits, C. Giordano, *J. Mater. Chem.*, 2011, 21, 17760-17764.
20. T. Ogawa, Y. Ogata, R. Gallage, N. Kobayashi, N. Hayashi, Y. Kusano, S. Yamamoto, K. Kohara, M. Doi, M. Takano, M. Takahashi, *Appl. Phys. Express*, 2013, 6, 073007/0 – 073007/3.
21. M.C. Roco, 2003, 14, 337-346.
22. R. Wrobel, W. Arabczyk, *J. Phys. Chem. A,* 2006, 110, 9219-9224.
23. W. Arabczyk, R. Wróbel, *Solid State Phenom*., 2003, 94,185-188.
24 R. Pelka, W. Arabczyk, *Polish Pat.* No. PL 216 582, 2014.
25. W. Arabczyk, R. Wróbel, W., *Solid State Phenom*., 2003, 94, 235-238.
26. I. Moszyńska, D. Moszyński, W. Arabczyk, *Przem. Chem.,* 2009, 88, no. 5, 526-529.
27. D. Moszyński, I. Moszyńska, *Przem. Chem.,* 2013, 92, no. 7, 1332-1335.
28. D. Moszyński, I. Moszyńska, W. Arabczyk, *Appl. Phys. Lett.*, 2013, 103, 253108/1-253108/4.
29. D. Moszyński, *J. Phys. Chem. C,* 2014, 118, 15440-15447.
30. W.P. Tong, N.R. Tao, Z.B. Wang, H.W. Zhang, J. Lu, K. Lu, *Scripta Mater.,* 2004, 50, 647-650.
31. M. Wohlschlögel, U. Welzel, E.J. Mittemeijer, *Appl. Phys. Lett.*, 2007, 91, 141901/1-141901/3.
32. W. Arabczyk, I. Jasińska, *Przem. Chem.,* 2006, 85, no. 2, 130-137.
33. J.R. Jennings, *Catalytic Ammonia Synthesis. Fundamentals and Practice*, Plenum Press, New York and London, 1991.
34. J.A. Burnett, H.Y. Allgood, J.R. Hall, *J. Ind. Eng. Chem.* 1953, 45, 393-403.
35. Z. Lendzion-Bieluń, R. Jędrzejewski, E. Ekiert, W. Arabczyk, *Appl. Catal. A: General* 2011, 400, 48-53.
36. W. Arabczyk, I. Jasińska, Z. Lendzion-Bieluń, *Catalysis Today,* 2011, 169, 93–96.
37. W. Arabczyk, I. Jasińska, K. Lubkowski, *React. Kinet. Catal. Lett*., 2004, 83, 385-392.
38. I. Jasińska, W. Arabczyk, *Chem. Pap.,* 2005, 59, 496-499.39. W. Arabczyk, U. Narkiewicz, D. Moszynski, *Langmuir*, 1999, 15, 5785-5789.
40. E.A. Ekiert, R. Pelka, K. Lubkowski, W. Arabczyk, *Pol. J. Chem. Tech.*, 2009, 11, No. 1, 28-33.
41. K. Lubkowski, B. Grzmil, W. Arabczyk, B. Michalkiewicz, A. Pattek-Janczyk, *Appl. Catal. A: General* 2007, 329, 137-147.
42. R. Pelka, K. Kiełbasa, W. Arabczyk, *J. Phys. Chem. C*, 2014, 118, 12, 6178-6185.
43. R. Pelka, W. Arabczyk, *Top. Catal.,* 2009, 52, 1506-1516.
44. W. Arabczyk, R. Pelka, I. Jasińska, *J. Nanomater.*, 2014, DOI: 10.1155/2014/473919.
45. D. Moszyński, K. Kiełbasa, W. Arabczyk, *Mater. Chem. Phys*., 2013, 141, 674-679.

46K. Kiełbasa, W. Arabczyk, *Pol. J. Chem. Tech.*, 2013, 15, 1, 97-101.
47. K. Kiełbasa, R. Pelka, W. Arabczyk, *J. Phys. Chem. A*, 2010, 114, 4531–4534.
48. N.I. Kardonina, A.S. Yurovskikh, A.S. Kolpakov, *Met. Sci. Heat Treat.*, 2011, 52, 457-467.
49. R. Pelka, W. Arabczyk, *Chem. Pap.,* 2011, 65, 198-202.